Journal of Applied Polymer Science

Supercritical Fluid CO_2 Processing and Counter Ion Substitution of Nafion® Membranes

Edward M. A. Guerrero-Gutiérrez, David Suleiman
Chemical Engineering Department, University of Puerto Rico, Mayagüez, Puerto Rico 00681-9000
Correspondence to: D. Suleiman (E-mail: David.Suleiman@upr.edu)

ABSTRACT: Nafion®-117 was exposed to supercritical fluid (SCF) CO_2 and a cation solution using two different approaches: first was processed with SCF CO_2, and then exchanged using six different cations: K^{+1}, Ca^{+2}, Ba^{+2}, Cu^{+2}, Fe^{+3}, and Al^{+3}. The second method performed the cation substitution first, followed by the SCF CO_2 processing. The resulting composite membranes were characterized using several techniques: thermogravimetric analysis (TGA), differential scanning calorimetry (DSC), Fourier transforms infrared spectroscopy (FT-IR), small angle X-ray scattering (SAXS), and X-ray diffraction (XRD). These techniques were used to identify the changes in the chemical and thermal properties of the membranes, as well as to evaluate changes in the resulting morphologies and crystallinities. Proton conductivity and methanol permeability were measured to understand how the different approaches promoted or inhibited the transport of certain substances through the membrane. Significant differences in their thermal, physical and transport properties were observed when Nafion® was processed with SCF CO_2 and exchanged with cations. © 2012 Wiley Periodicals, Inc. J. Appl. Polym. Sci. 000: 000–000, 2012

KEYWORDS: batteries and fuel cells; membranes; spectroscopy; thermogravimetric analysis (TGA); X-ray

Received 3 September 2012; accepted 5 October 2012; published online
DOI: 10.1002/app.38689

INTRODUCTION

Nonfluorinated polymers, like sulfonated poly(styrene-isobutylene-styrene),[1] sulfonated aromatic poly(etheretherketone),[2] sulfonated polyarylenethioether sulfones, poly(arylenene ether sulfone)[3] and fluorinated polymers like poly(arylene ether benzonitrile) containing hexafluoroisopropylidene diphenol[4] have been studied as proton exchange membranes (PEMs) for direct methanol fuel cells (DMFC). Unfortunately, even today most of these PEMs have either low proton conductivity (σ) or high methanol permeability limiting their performance in DMFC. Nafion® is a sulfonated fluoropolymer that is commonly used in DMFC. This membrane consists of a polytetrafluoroethylene backbone and regularly spaced long perfluorovinyl ether pendant side chains terminated by a sulfonate ionic group.[5] Nafion® remains the standard in DMFC, because it has very high proton conductivity and excellent thermal and mechanical properties; unfortunately, it also has higher than desired methanol permeability leading to the well-known methanol cross-over limitation.[6]

Different researches have investigated the incorporation of acidic inorganic–organic fillers to Nafion® with the objective of obtaining Nafion® membranes with lower methanol permeability; however, some of these composite Nafion® membranes decreased the proton conductivity similar to the reduction in methanol permeability.[6–8]

Supercritical fluid (SCF) processing with CO_2 has been another alternative used to modify the morphology of fluoroelastomers. SCF CO_2 possesses gas-like mass transport properties (e.g., high diffusivity and low viscosity) and liquid-like densities to easily penetrate the membrane, while aligning functional groups according to physico-chemical affinities. NMR studies suggest specific interactions between ^{19}F isotope and supercritical CO_2 which may support the high solubility of many fluorocarbon polymers in SCF CO_2.[9]

A limited number of studies have evaluated the effect of SCF CO_2 processing on polymer membranes. Akin and Temelli[10] processed two commercial polyamide membranes using SCF CO_2. They found out that there was a reorganization of the polymeric network induced by the processing time and depressurization. Su et al.[11] prepared perfluorosulfonic acid membranes and then treated them with SCF CO_2. Their membranes showed a change in the size of the ion cluster and the relative crystallinity, which led to a reduction in the methanol permeability. Gribov et al.[12] incorporated zeolite (Fe-silicalite-1) to Nafion®-115 assisted by SCF CO_2. Their membranes had lower methanol permeability than nonprocessed Nafion®-115. Pulido

and Suleiman[13] modified the morphology of Nafion®-117 using SCF CO_2 with different cosolvents. A significant reduction in the methanol permeability was observed with a smaller loss of proton conductivity.

Two major factors influence the transport properties throughout polymer membranes, morphology and physicochemical interactions. SCF CO_2 processing seems to have a strong influence in the morphology of perfluorosulfonic membranes. Therefore, the goal of this investigation was to evaluate if the changes in the morphology of Nafion®-117 when exposed to SCF CO_2 and different metallic cations affected their transport, thermal and physical properties and to determine if the order of the processing affected these properties. The selection of cations included the evaluation of different size and electronegativity within the same group (e.g., Ca^{+2} and Ba^{+2}) and cations of different number of valence electrons within the same period (e.g., K^{+1}, Ca^{+2}, Fe^{+3}, and Cu^{+2}). In addition, Al^{+3} was evaluated since a previous study showed changes in the thermogravimetric properties of Nafion®-117,[14] but lacked the evaluation of transport properties. The SCF processed membranes were then characterized for methanol permeability, proton conductivity, and water swelling; the results were explained with some additional materials characterization techniques (e.g., FT-IR, TGA, DSC, SAXS, and XRD).

EXPERIMENTAL

Materials

Ultrahigh purity CO_2 (99.998% purity) was acquired from Linde Gas Puerto Rico. Nafion®-117 (from now on Nafion®) was obtained from Ion Power. Other chemicals used include: potassium chloride -KCl-, (Sigma–Aldrich, anhydrous powder, 99.99%), calcium chloride anhydrous -$CaCl_2$-, (Acros Organic, anhydrous powder, 96%), barium chloride -$BaCl_2$-, (Fisher Scientific, anhydrous powder, 99.99%), cooper chloride -$CuCl_2$- (Sigma–Aldrich, anhydrous powder, 99.99%), aluminum chloride -$AlCl_3$- (Acros Organic, extra pure anhydrous, 99.99%), ferric chloride -$FeCl_3$- (Sigma–Aldrich, anhydrous powder, 99.99%), hydrogen peroxide -H_2O_2- (3 wt % solution in water stabilized) and sulfuric acid -H_2SO_4- (Sigma–Aldrich, ACS reagent, 95.0–98.0%) were employed as received.

Sample Preparation

Nafion® membranes used in this study were first pretreated to convert them into their acid form using the following procedure: the membrane was first treated with a hydrogen peroxide solution (3 wt %) during 1 h at 80°C, and then washed with deionized water also for 1 h at 80°C. After the initial wash, the membrane was protonated with sulfuric acid (1 *M*), and finally washed with deionized water; both of those steps for 1 h at 80°C each.

Nafion® membranes were processed with SCF CO_2 at 40°C and 100 bar during 1 h in a supercritical fluid extractor (Isco SFX 2-10). The SCF CO_2 flowed parallel to the membrane during the experimentation. After the SCF processing, the membrane was submerged in a 1 *M* solution of KCl, $CaCl_2$, $BaCl_2$, $CuCl_2$, $AlCl_3$, or $FeCl_3$ depending on the desired cation for 48 h. The resulting cation-exchanged Nafion® membranes were washed using deionized water and dried at 60°C during 24 h.

Thermogravimetric Analysis (TGA)

The thermal degradation behavior and water loss for each membrane was determined using a Mettler Toledo 851e instrument. In each experiment, polymer samples weighting ~ 5–10 mg were used. Degradation temperatures were determined after heating the polymer samples to 800°C at 10°C min^{-1} under a nitrogen atmosphere.

Differential Scanning Calorimetry (DSC)

The thermo physical properties were determined using differential scanning calorimetry (DSC). A Texas Instrument DSC Q2000 unit was used for this purpose. In each experiment, polymer samples weighting ~ 5–10 mg were used. The samples were pre-heated from 30 to 110°C at 10°C min^{-1} and then cooled down from 110 to −90°C at 5°C min^{-1}. Phase transitions (T_g) and melting points for each membranes were determined after heating the polymer samples from −90 to 350°C at 10°C min^{-1} under a nitrogen atmosphere.

Fourier Transform Infrared Spectroscopy

Fourier-transform infrared (FT-IR) spectroscopy uses vibrational energy to characterize organic compounds. An attenuated total reflectance (ATR) cell was used with an FT-IR (Varian 800 FT-IR) to analyze the peak position and intensities of the perfluorocarbon backbone, the perfluoroether segment and the sulfonic groups, before and after processing with SCF CO_2 and cation substitution. Nafion® membranes were clamped on the ATR cell and all infrared spectra were collected using 64 scans, 4 cm^{-1} resolution and a range of 600–4000 cm^{-1}.

Small Angle X-ray Scattering (SAXS)

The morphology of the membranes was studied using small angle X-ray scattering (SAXS). SAXS was performed on a beamline X27C. Two-dimensional scattering patterns were collected on a pinhole-collimated system using Fujitsu image plates and read by a Fujitsu BAS 200 image plate reader. The SAXSQuant software® was used to reduce two dimensional data to one-dimensional intensity versus scattering vector (q) plots after background subtraction by circular averaging. The X-ray wavelength employed was 1.6 Å. The calibration standard was silver behenate and the sample distance to the detector was 210 cm.

Methanol Liquid-Phase Permeability

The methanol liquid-phase permeability was measured using a side-by-side glass diffusion cell discussed in detail elsewhere.[13] One side contained the permeant (e.g., methanol) in a 2*M* methanol–water solution, while the other side only contained deionized water. The concentration of the compound that permeated through the membrane was determined using a gas chromatograph (GC) equipped with a thermal conductivity detector (TCD) (Shimadzu GC-8). First a calibration curve was created, and then measurements were determined after different times. The liquid permeability was obtained from the continuity equation for diffusion in plane geometry[15] [eq. (1)]:

$$C_B(t) = \frac{PC_A A}{V_b L}\left(t - \frac{L^2}{6D}\right) \quad (1)$$

where C_A (mol cm^{-3}) is the methanol concentration (permeant), C_B (mol cm^{-3}) is the concentration of the compound that

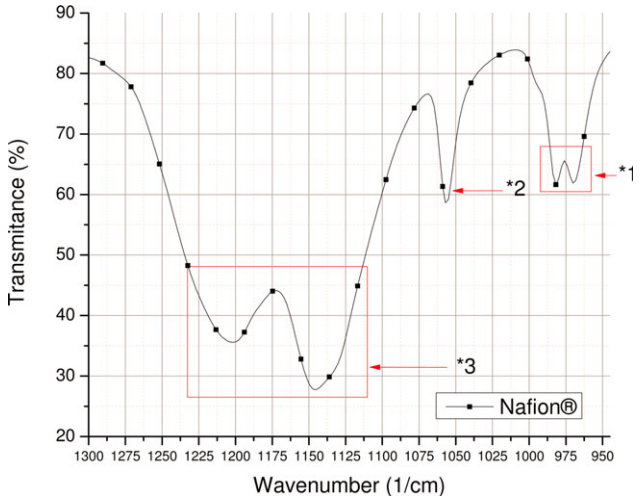

Figure 1. FTIR spectra for Nafion® (—■—). [Color figure can be viewed in the online issue, which is available at wileyonlinelibrary.com.]

permeated thought the membrane after different times, L is the membrane thickness, V_b the volume of the receptor compartment (0.39 cm^3), A the diffusional cross-sectional area of the membrane (0.64 cm^2), and P the permeability (cm^2 s^{-1}). The permeability (P) was determined from the slope of the concentration $C_B(t)$ versus time.[16]

Proton Conductivity

The proton conductivity (σ) of each membrane was measured normal to the plane using AC electrochemical impedance spectroscopy (EIS). The measurements were carried out on an AC Solartron impedance system: 1260 impedance analyzer, 1287 electrochemical interface, Zplot software. The range of frequency and voltage used were from 0.1 Hz to 1.0 MHz and 10–15 mV, respectively at room temperature and 100% relative humidity. The membranes were first immersed in an excess of deionized water at 25°C before the experimentation during 24 h. The proton conductivity was calculated from the impedance data, using the following relation [eq. (2)][17]:

$$\sigma = \frac{L}{R_\Omega A} \tag{2}$$

where L is the distance between electrodes (0.3 cm), A (cm^2) is the area obtained from the product of the thickness and the width of the membrane. R_Ω was obtained from the low intersect of the high frequency semicircle (Nyquist plot) on the complex impedance plane with the real component of the impedance axis (Re(z)).

X-ray Diffraction (XRD)

The crystallinity of the membranes was obtained using an X-ray diffraction (XRD) instrument (Bruker D8 Discover with GADDS). The X-ray wavelength employed was 1.54 Å and the 2-theta range was from 20° to 90°. No previous sample preparation was performed before the measurements, including humidity pretreatment.

Water Swelling

Water absorption or water swelling in the membranes was measured immersing each membrane in an excess of deionized water at 25°C. The weight of the sample initially dried at 75° for 24 h in an oven was originally recorded, as well as the weight of the membrane after immersion in water. The weights of the wet membranes were measured after different time intervals until swelling equilibrium was reached. Each reported result represents the average of at least three repetitions.

RESULTS AND DISCUSSIONS

FT-IR Spectroscopy

Figure 1 presents the FT-IR spectrum of Nafion®, three distinctive regions can be observed in this figure. The sulfonic group appears as a medium band around 1055 cm^{-1} (*2). This band was caused by an asymmetric stretching vibration of the sulfonated functional group attributed to the S=O bond. The polymer backbone (—CF_2—) has a strong band from 1100 to 1300 cm^{-1} (*3) and the ether linkage (—O—) from the perfluorovinyl ether appears around 980 cm^{-1} (*1).

Figure 2 shows the FT-IR spectrum for Nafion® and Nafion® processed with SCF CO_2 with cation-exchanged K^{+1}, Ca^{+2}, Cu^{+2} [A], and Fe^{+3}, Ba^{+2}, Al^{+3} [B]. Nafion® processed with SCF CO_2 and cation-exchanged presented significant reductions in their intensities in all regions (*1, *2, and *3). These results can represent the interaction of the cation-exchanged and the SCF processing with all the groups mentioned, not with a specific group. FT-IR results for cation substituted sulfonated poly(styrene-isobutylene-styrene) show that the cations interact with the sulfonic group only shifting the asymmetric S=O band *2[18]; this is not the case for Nafion®.

Table I shows the reduction or increase on the transmittance for each peak in the FTIR spectra. The intensity increased when Nafion® is processed with SCF CO_2, but decreased when exchanged with all the cations. This behavior is the same for

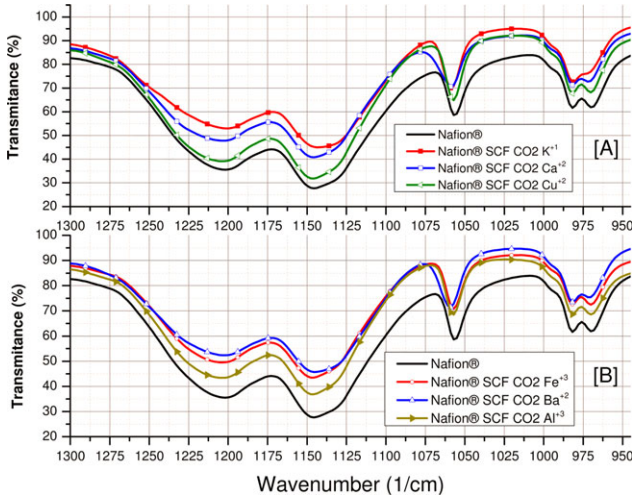

Figure 2. FTIR for Nafion® and Nafion® processed with SCF CO_2 and cation-exchanged: K^{+1} (—■—), Ca^{+2} (—□—), Cu^{+2} (—◁—) [A] and Fe^{+3}(—○—), Ba^{+2} (—△—), Al^{+3} (—▷—) [B]. [Color figure can be viewed in the online issue, which is available at wileyonlinelibrary.com.]

Table I. Reduction or Increase on Transmittance Nafion® Processed with SCF CO_2 and with Cation-Exchanged

Sample	Polymer backbone (CF_2)		Ether linkage (—O—) (%)	Sulfonic group (%)	Effect in the intensity
	Peak 1 (%)	Peak 2 (%)			
Nafion® SCFCO_2	14	10	4	6	Higher
Nafion® SCF CO_2 K^{+1}	60	46	17	18	Lower
Nafion® SCF CO_2 Ca^{+2}	46	35	15	19	Lower
Nafion® SCF CO_2 Ba^{+2}	64	46	18	20	Lower
Nafion® SCF CO_2 Cu^{+2}	14	10	10	10	Lower
Nafion® SCF CO_2 Al^{+3}	32	21	11	15	Lower
Nafion® SCF CO_2 Fe^{+3}	55	39	18	20	Lower

Nafion® exchanged with cations first and then processed with SCF CO_2. Other experiments are presented ahead to understand the impact of the cation substitution in the membranes.

Water Swelling

The water absorbed by Nafion® is related to the molecular structure of the ionomer domains, and the morphology of the membrane.[19] Figure 3 presents the percent of water swelling vs. time for each of the membranes studied. Equilibrium for all Nafion® membranes was obtained after 70 h of the membranes submerged in water.

Figure 4 shows the water swelling comparison between Nafion® processed with SCF CO_2 first and then cation-exchanged and Nafion® cation-exchanged first and then processed with SCF CO_2. Unprocessed Nafion® obtained the highest water swelling and this was reduced when the membrane was processed with SCF CO_2. This can be attributed to the rearrangement of the sulfonic groups, the polymer backbone and the perfluorovinyl ether after exposure to the SCF CO_2.

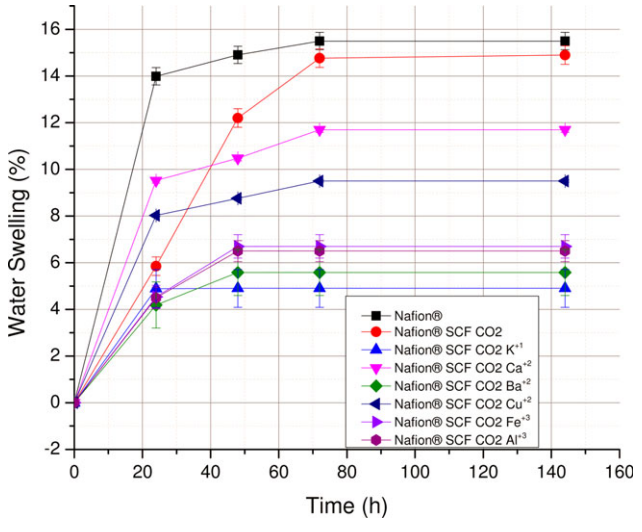

Figure 3. Water Swelling for Nafion® (—■—) processed with SCF CO_2 (—●—) and then cation-exchanged. K^{+1} (—▲—), Ca^{+2} (—▼—), Ba^{+2} (—◆—), Cu^{+2} (—◀—), Fe^{+3} (—▶—), Al^{+3} (—●—). [Color figure can be viewed in the online issue, which is available at wileyonlinelibrary.com.]

The incorporation of cations into the membrane produced even lower but unique water swelling for each of the cations studied. The incorporation of cations inverted all ionic domains toward a more hydrophobic environment.[20] Nafion® processed with SCF CO_2 and exchanged with K^{+1} obtained the lowest percent of water swelling and Nafion® processed with SCF CO_2 and exchanged with Ca^{+2} produced the highest amount of water swelling for all the cations studied. This behavior could be attributed to a complex arrangement in their morphologies due to the cation substitution and SCF CO_2 processing. This will be further evaluated with the additional materials characterization studies. Table II summarizes the water swelling results for these experiments.

Thermogravimetric Analysis (TGA)

Figure 5(a) shows the TGA curve for unprocessed Nafion® observing five degradation temperatures, the first one corresponds to water absorbed inside the membrane, the second degradation region represents the sulfonic group, and all the other degradations represent different fluorocarbon backbones.[21]

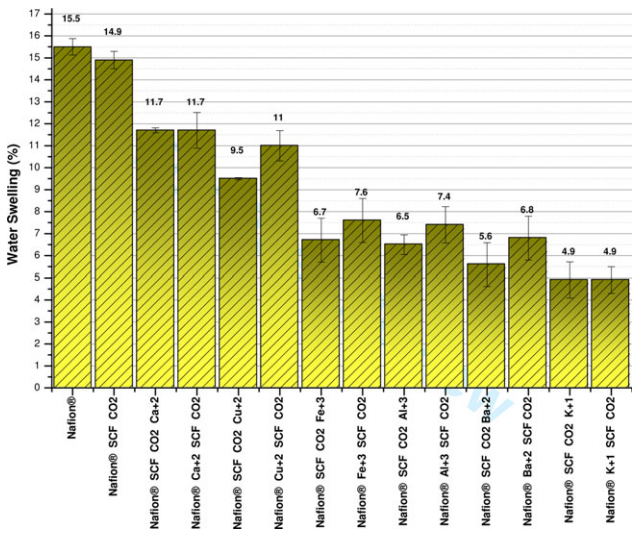

Figure 4. Comparison between water swelling for Nafion® processed with SCF CO_2 and then cation-exchanged and Nafion® cation-exchanged and then processed with SCF CO_2. [Color figure can be viewed in the online issue, which is available at wileyonlinelibrary.com.]

Table II. Water Swelling for Nafion® Membranes

Membrane	Water swelling (%)
Nafion®	15.5 ± 0.4
Nafion® SCF CO_2	14.9 ± 0.4
Nafion® SCF CO_2 Ca^{+2}	11.7 ± 0.1
Nafion® Ca^{+2} SCF CO_2	11.7 ± 0.8
Nafion® SCF CO_2 Cu^{+2}	9.5 ± 0.04
Nafion® Cu^{+2} SCF CO_2	11.1 ± 0.7
Nafion® SCF CO_2 Fe^{+3}	6.7 ± 1.2
Nafion® Fe^{+3} SCF CO_2	7.6 ± 1.0
Nafion® SCF CO_2 Al^{+3}	6.5 ± 0.4
Nafion® Al^{+3} SCF CO_2	7.4 ± 0.8
Nafion® SCF CO_2 Ba^{+2}	5.6 ± 1.0
Nafion® Ba^{+2} SCF CO_2	6.8 ± 1.6
Nafion® SCF CO_2 K^{+1}	4.9 ± 0.8
Nafion® K^{+1} SCF CO_2	4.9 ± 0.6

Nafion® processed with SCF CO_2 presented two regions in the TGA that remained unchanged, but the fluorocarbon backbone only showed one degradation temperature at 465°C [Figure 5(b)]. This behavior confirmed the interaction between the fluorocarbon backbone and the perfluorovinyl ether of Nafion® with SCF CO_2.

When Nafion® processed with SCF CO_2 was exposed to different cations; different degradation temperatures were obtained depending on the cation exchanged. Table III shows the exact degradation temperatures for each of the cations studied. A unique feature was observed for potassium-substituted Nafion®; although its structure degraded at 459.10°C, its second degradation region, (corresponding to the sulfonic group), is absent. This suggests that potassium interacts directly with the sulfonic groups. In addition, the fluorocarbon backbone and the ether linkage from the perfluorovinyl ether changed their thermal degradation [Figure 6(a)]. The thermal stability of Nafion® significantly improved after the cation-substitution of the membrane using potassium, calcium and barium. For those cations, the second degradation (sulfonic group) was absent; suggesting that the cation interacted with the sulfonic group, but each cation presented a different and unique behavior with the other degradation regions. Calcium increased the thermal stability of Nafion® even further than potassium and barium.

The thermal stability of Nafion® was adversely affected when exchanged with aluminum, iron and copper. The aluminum cations gave rise to a catalytic decomposition of the perfluorovinyl ether side chains of Nafion®.[14] During this step of the

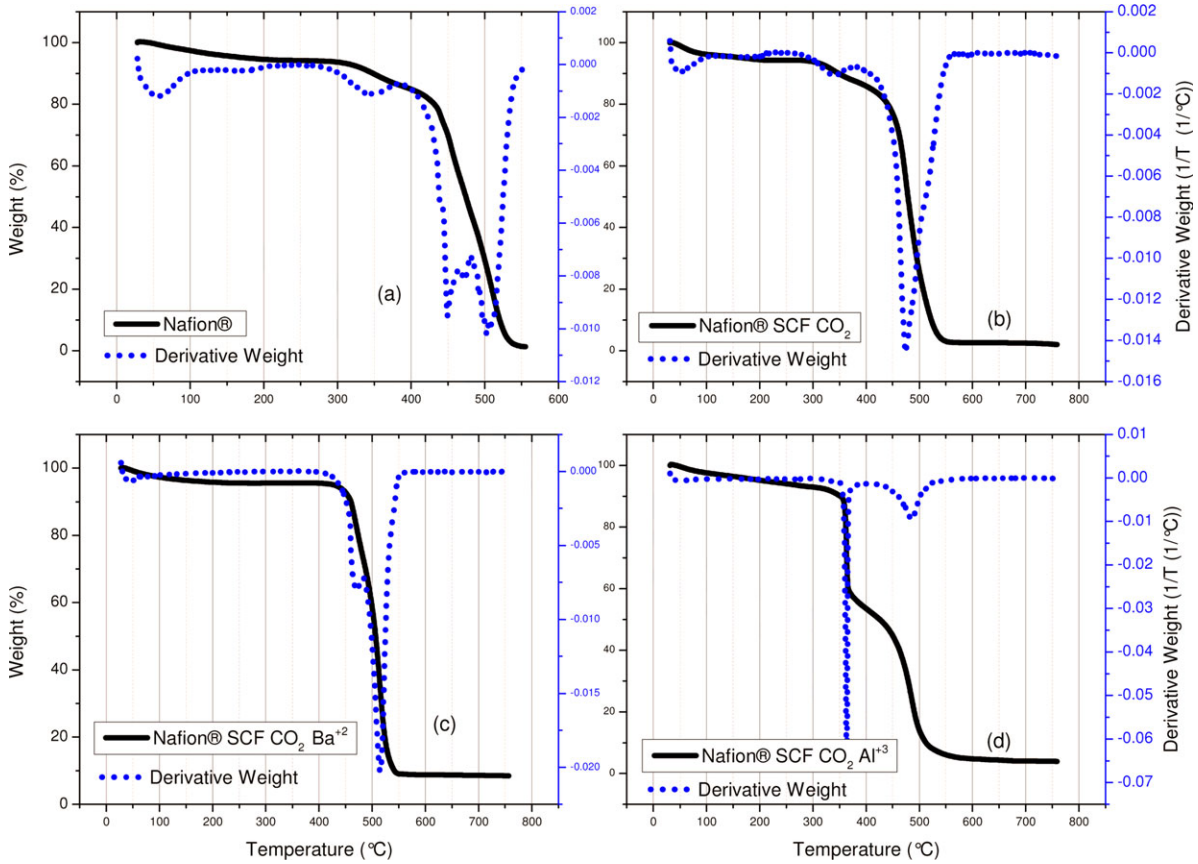

Figure 5. Thermogravimetric analysis (TGA) for Nafion® (a) processed with SCF CO_2 (b) and processed with SCF CO_2 first and then the cation exchanged [Ba^{+2} (c) and Al^{+3} (d)]. Derivative weight curves (short dot line). [Color figure can be viewed in the online issue, which is available at wileyonlinelibrary.com.]

Table III. Degradation Temperatures for Nafion® Processed with SCF CO_2 First and then Cation-Exchanged

Membrane	1st degradation (°C)	2nd degradation (°C)	3rd degradation (°C)	4th degradation (°C)	5th degradation (°C)
Nafion®	65	330	450	470	500
Nafion® SCF CO_2	55	340	Absent	465	Absent
Nafion® SCF CO_2 K^{+1}	Absent	Absent	459.10	Absent	533.02
Nafion® SCF CO_2 Ca^{+2}	55	Absent	Absent	479.44	Absent
Nafion® SCF CO_2 Ba^{+2}	Absent	Absent	Absent	469.54	514.78
Nafion® SCF CO_2 Cu^{+2}	Absent	360.38	395.85	Absent	511.64
Nafion® SCF CO_2 Al^{+3}	Absent	350	Absent	475	Absent
Nafion® SCF CO_2 Fe^{+3}	Absent	335.54	423.22	Absent	Absent

decomposition, one or both of the two ether bonds are broken and a series of small fluorocarbon molecules are formed, which leave primarily the fluorocarbon backbone main chains.[14] Part of the fluorocarbon backbone and sulfonic group suffered thermal degradation below 350°C and the remaining polymer chain was degraded up to 475°C [Figure 5(d)].

Figure 6(c,d) shows the TGA curve for Nafion® SCF CO_2 exchanged with iron and copper. In the case of copper, the sulfonic group degraded at 360.38°C and the fluorocarbon backbone was thermally unstable and began the thermal degradation at 395.85°C. Nafion® SCF CO_2 exchanged with Fe^{+3} had a small loss weight to 335.54°C (sulfonic group region), but the fluorocarbon backbone was also thermally unstable. Major weight loss for this cation occurred at 423.22°C. Nafion® membranes exchanged first with the cations and then processed with SCF CO_2 showed the same behavior than Nafion® processed with SCF CO_2 and then cation-exchanged, but had a small difference in the degradation temperatures (Table IV).

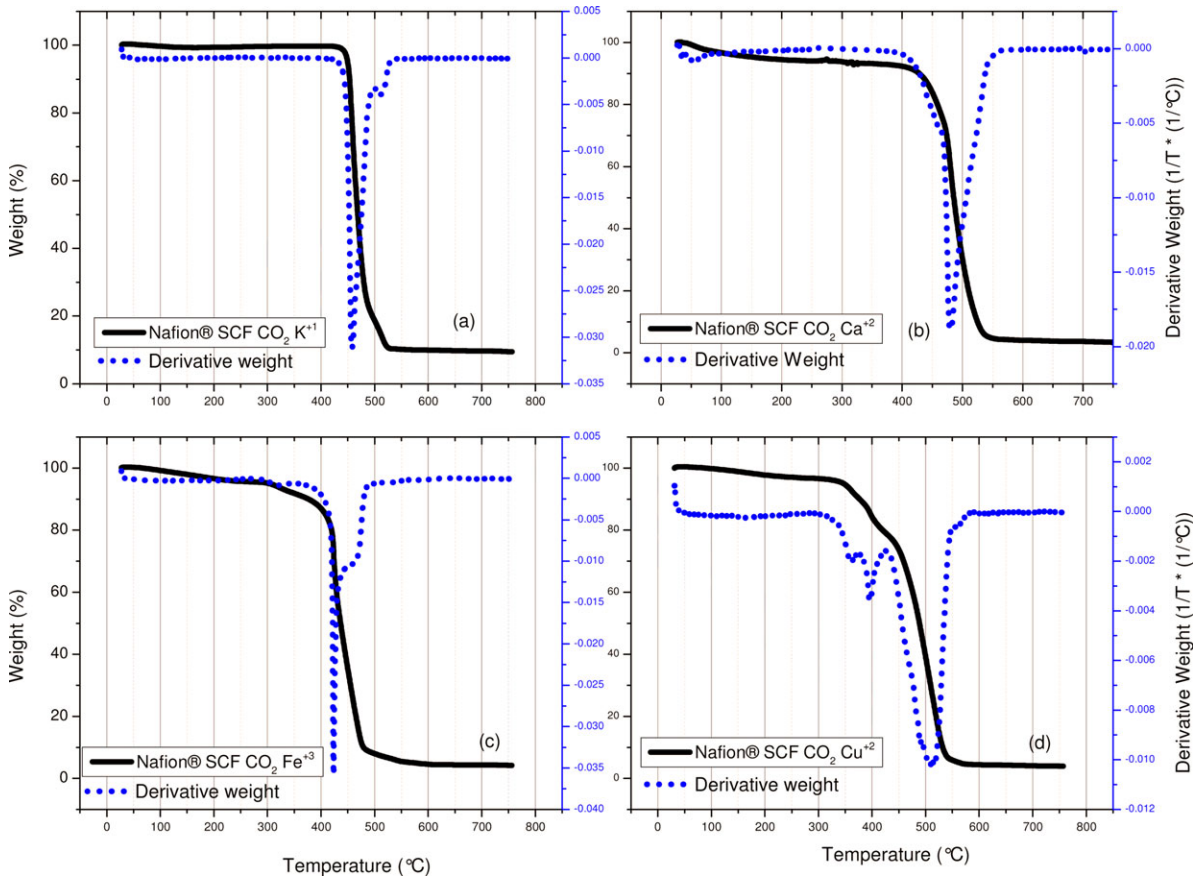

Figure 6. Thermogravimetric analysis (TGA) for Nafion® processed with SCF CO_2 first and then the cation exchanged [K^{+1} (a), Ca^{+2} (b), Fe^{+3} (c) and Cu^{+2} (d)]. Derivative weight curves (short dot line). [Color figure can be viewed in the online issue, which is available at wileyonlinelibrary.com.]

Table IV. Degradation Temperatures for Nafion® Exchanged with Cation First and then Processed with SCF CO_2

Membrane	1st degradation (°C)	2nd degradation (°C)	3rd degradation (°C)	4th degradation (°C)	5th degradation (°C)
Nafion®	65	330	450	470	500
Nafion® SCF CO_2	55	340	Absent	465	Absent
Nafion® K^{+1} SCF CO_2	Absent	Absent	459.92	absent	527.13
Nafion® Ca^{+2} SCF CO_2	Absent	Absent	Absent	489.19	Absent
Nafion® Ba^{+2} SCF CO_2	Absent	Absent	Absent	468.55	512.40
Nafion® Cu^{+2} SCF CO_2	Absent	360.52	397.97	Absent	513.76
Nafion® Al^{+3} SCF CO_2	Absent	354.51	Absent	492.35	Absent
Nafion® Fe^{+3} SCF CO_2	Absent	340.39	421.72	Absent	Absent

Differential Scanning Calorimetry (DSC)

Figure 7 present DSC curves for unprocessed Nafion® and Nafion® processed with SCF CO_2. Unprocessed Nafion® presents two endothermic peaks; the first thermal transition at 156.8°C corresponds to the transition of the ionic domains, while the peak at higher temperature (191.7°C) is attributed to the crystalline regions.[22] Nafion® processed with SCF CO_2 also presents the two endothermic peaks, the first at 154.82°C and the second peak at 194.58°C. The changes in temperature with respect to unprocessed Nafion®, are related to the energy needed to overcome the crystalline bonding forces and changes in the molecular conformation of the chains in the polymer.[23]

Figure 8 presents the comparison between DSC for unprocessed Nafion®, Nafion® processed with SCF CO_2 [A] and Nafion® processed with SCF CO_2 and then cation-exchanged [B]. The incorporation of cations to the membrane produced unique DSC curves for each of the cations studied. Nafion® processed with SCF CO_2 and exchanged with potassium presented a difference in both the energy and temperature required to produce the endothermic transitions. The endothermic transitions for the ionic cluster and crystalline regions shifted towards higher temperature and the energy required for the endothermic transition of the crystalline region presented the highest reduction for all the cations in comparison with unprocessed Nafion®. The other cations also presented changes in the energy required to produce the endothermic transitions but showed a reduction in temperature. Nafion® SCF CO_2 Ca^{+2} presented only one endothermic peak; in this case the incorporation of the cation reduced the temperature of the crystalline region and the ionic cluster to a single temperature. The other cations presented two endothermic peaks. Table V summarizes the endothermic transition temperatures and their corresponding energies for the Nafion® membranes studied.

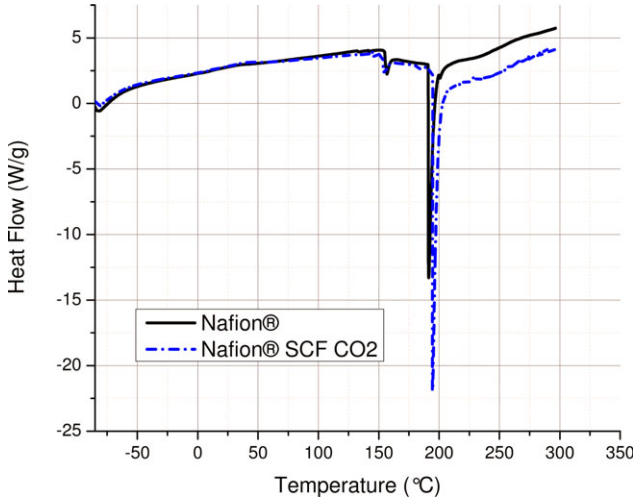

Figure 7. DSC for Nafion® (Straight line) and Nafion® processed with SCF CO_2 (short dash dot line). [Color figure can be viewed in the online issue, which is available at wileyonlinelibrary.com.]

Small Angle X-ray Scattering (SAXS)

SAXS profiles for Nafion® membranes are shown in Figures 9 and 10. Unprocessed Nafion® shows three characteristic regions in the SAXS profile: (1) corresponds to the matrix knee. The intensity of this region depends on the crystallinity of the membrane[24]; (2) the ionomer peak (this region plays an important

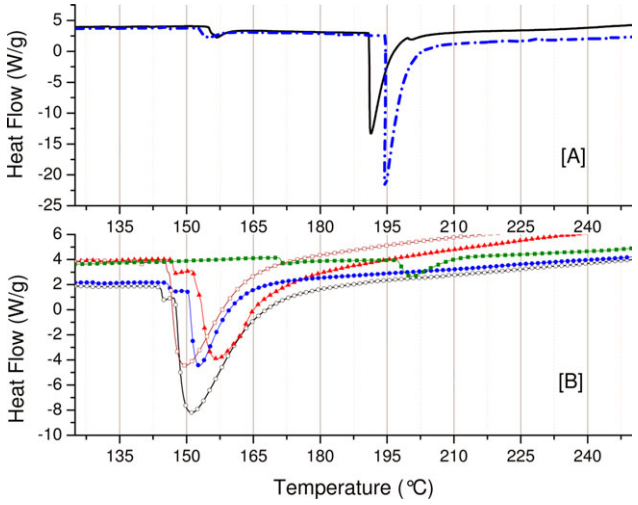

Figure 8. Comparison between DSC for Nafion® (Straight line), Nafion® processed with SCF CO_2 (short dash dot line) [A] and Nafion® processed with SCF CO_2 and then cation-exchanged [B]. K^{+1} (—■—), Ca^{+2} (—□—), Ba^{+2} (—●—), Fe^{+3} (—○—), Al^{+3} (—▲—). [Color figure can be viewed in the online issue, which is available at wileyonlinelibrary.com.]

Table V. Endothermic Transition Temperatures and Corresponding Energies for Nafion® Membranes

Membrane	$T_{transition}$ (°C) (1)	ΔH (J g^{-1}) (1)	$T_{transition}$ (°C) (2)	ΔH (J g^{-1}) (2)
Nafion®	156.8	4.7	191.7	60.7
Nafion® SCF CO_2	154.8	2.8	194.5	70.7
Nafion® SCF CO_2 Cu^{+2}	154.4	43.9	Absent	Absent
Nafion® Cu^{+2} SCF CO_2	152.3	2.6	198.2	83.7
Nafion® SCF CO_2 Ca^{+2}	149.9	64.6	Absent	Absent
Nafion® Ca^{+2} SCF CO_2	149.3	51.3	Absent	Absent
Nafion® SCF CO_2 Ba^{+2}	146.7	0.75	152.8	34.8
Nafion® Ba^{+2} SCF CO_2	149.7	1.9	156.2	35.99
Nafion® SCF CO_2 K^{+1}	171.9	1.01	200.8	9.96
Nafion® K^{+1} SCF CO_2	163.8	0.43	178.9	7.4
Nafion® SCF CO_2 Al^{+3}	147.5	1.15	156.5	54.1
Nafion® Al^{+3} SCF CO_2	151.5	3.2	194.9	89.6
Nafion® SCF CO_2 Fe^{+3}	144.8	0.61	151.0	94
Nafion® Fe^{+3} SCF CO_2	149.2	2.76	183.1	93.8

role in the transport of certain compounds, like methanol or protons, through the membrane) and (3), correspond to large q-vectors, the ultra low angle area.[5]

Nafion® processed with SCF CO_2 presented changes in regions *1, *2, and *3 in the SAXS profile with respect to unprocessed Nafion® (Figure 9). This behavior agrees with the results obtained with FTIR, where the different intensities from FTIR spectra were related with the interaction between the perfluorocarbon backbone and the ionomer group with the SCF CO_2. The SAXS results also agree with the DSC experiments where a different ionic configuration and crystallinity was obtained upon SCF CO_2 processing.

Nafion® membranes processed with SCF CO_2 and crosslinked with cations showed different positions for the ionomer peak with respect to unprocessed Nafion® (Figure 10). The positions

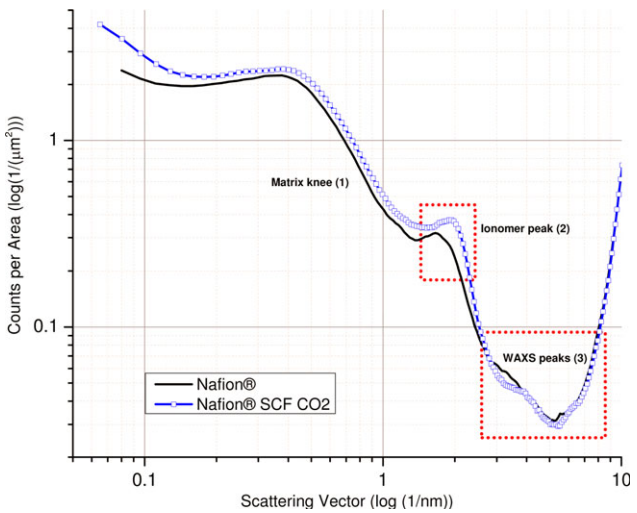

Figure 9. SAXS profile for Nafion® (straight line) and Nafion® processed with SCF CO_2 (—□—). [Color figure can be viewed in the online issue, which is available at wileyonlinelibrary.com.]

of these peaks for some cations obtained by the scattering vector appear from 1.58 to 2.04 nm^{-1}. In other cases this peak disappears due to the interaction between the cation and the ionomer group (Figure 10). Combining Bragg's law with the scattering vector (Q) obtained from the SAXS plot, the interstitial distance for the ionic domains was obtained. Table VI shows the Bragg's distance for the ionomer peak for Nafion® and Nafion® processed with SCF CO_2 and then exchanged with cations. The variations in the ionomer peak agree with the previously presented DSC results, where a new and unique ionic configuration was obtained depending on the SCF CO_2 processing and the cation selected.

Another important parameter that was obtained from the SAXS data is the radius of gyration (R_g). For polymers, this parameter represents the dimension of a polymer chain and can be used to evaluate changes with the variables studied. This parameter was obtained using the Guinier equation, which provides the relation between R_g, the intensity in a SAXS profile and the scattering vector (Q). R_g was estimated using the slope of the linear relationship between Ln(I(Q)) and Q^2.[25] Nafion® processed with SCF CO_2 presented a reduction in the radius of gyration of 2.29% with respect to unprocessed Nafion®. The incorporation of cations into the Nafion® membrane produced unique R_gs. Nafion® processed with SCF CO_2 and exchanged with cations had an even greater reduction in the radius of gyration. Nafion® SCF CO_2 with Al^{+3} reduced R_g by 5% with respect to unprocessed Nafion®. The incorporation of barium reduced this parameter the most (54%) and was the lowest R_g for all the membranes studied. The R_g results for Nafion® processed with SCF CO_2 and cation-exchanged are summarized in Table VII. SCF CO_2 processing and the incorporation of cation substitution compacted all the polymeric chains, creating a new molecular configuration. These results agree with the water swelling, DSC and TGA experiments, where a new configuration for the ionic domain and the perfluorocarbon backbone was obtained depending on the processing and the cation selected.

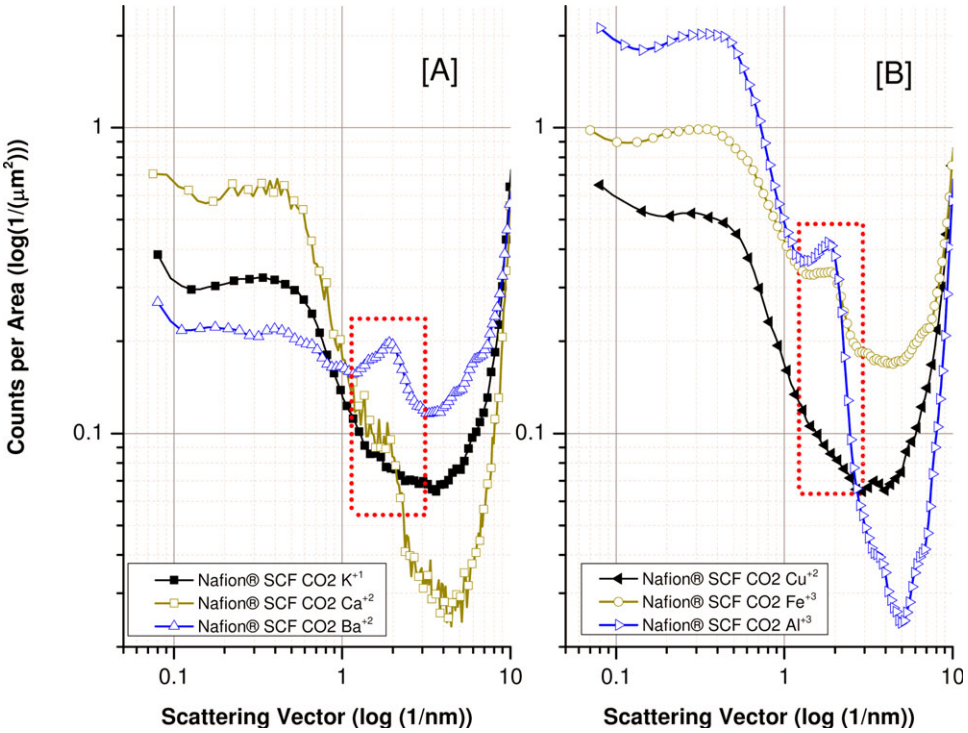

Figure 10. SAXS profile Nafion® processed with SCF CO_2 and cation exchanged: K^{+1} (—■—), Ca^{+2} (—□—), Ba^{+2} (—△—) [A], and Cu^{+2} (—◀—), Fe^{+3} (—○—), Al^{+3} (—▷—) [B]. [Color figure can be viewed in the online issue, which is available at wileyonlinelibrary.com.]

X-ray Diffraction (XRD)

X-ray diffraction measurements were performed to evaluate changes in the crystallinity of the Nafion® membranes. Figure 11 shows the XRD patterns of Nafion® membranes processed with SCF CO_2 and exchanged with different cations. Nafion® presents a large peak at the 2θ angle of 17°, which is formed by the superposition of amorphous scattering at 16° in the polymeric chain and the crystalline scattering at 17.5°.[26] A wide peak appears at the 2θ angle of 38°–39° (amorphous region).[26] Crystallinity values were obtained using the area of the deconvoluted crystalline peak divided by the total area (crystalline plus amorphous peaks).

The crystallinity of Nafion® processed with SCF CO_2 increased 11% compared with unprocessed Nafion®. This behavior agrees with the results in the literature, where perfluorosulfonic membranes increased their crystallinity after processing with SCF CO_2.[11,12,27]

The incorporation of cations into the membrane produced changes in the intensity of both peaks in the XRD pattern. The crystallinity of Nafion® membrane increased or decreased depending on the cation-exchanged. Figure 12 presents a frontal view of the XRD patterns for Nafion® membranes. The incorporation of potassium reduced the crystallinity of Nafion® by 12% and was the lowest value for all the membranes studied.

Table VI. Bragg Distance for Ionomer Peak for Nafion® Membranes

Sample	d_{bragg} (nm)	Atomic radius of the cation (nm)
Nafion®	3.97	-
Nafion® SCF CO_2	3.47	-
Nafion® SCF CO_2 Ca^{+2}	3.53	0.18
Nafion® SCF CO_2 Cu^{+2}	Absent	0.135
Nafion® SCF CO_2 Ba^{+2}	3.53	0.215
Nafion® SCF CO_2 Fe^{+3}	3.08	0.14
Nafion® SCF CO_2 Al^{+3}	3.69	0.125
Nafion® SCF CO_2 K^{+}	Absent	0.22
Nafion® Ca^{+2} SCF CO_2	3.29	0.18
Nafion® Ba^{+2} SCF CO_2	3.81	0.215
Nafion® Cu^{+2} SCF CO_2	3.98	0.135
Nafion® Al^{+3} SCF CO_2	3.90	0.125
Nafion® Fe^{+3} SCF CO_2	4.39	0.14
Nafion® K^{+} SCF CO_2	Absent	0.22

Table VII. Radius of Gyration for Nafion® Membranes

Membrane	Radius of Gyration (nm)
Nafion®	2.66
Nafion® SCF CO_2	2.59
Nafion® SCF CO_2 K^{+1}	1.89
Nafion® SCF CO_2 Ca^{+2}	2.36
Nafion® SCF CO_2 Ba^{+2}	1.22
Nafion® SCF CO_2 Cu^{+2}	2.20
Nafion® SCF CO_2 Fe^{+3}	1.83
Nafion® SCF CO_2 Al^{+3}	2.51

Applied Polymer SCIENCE

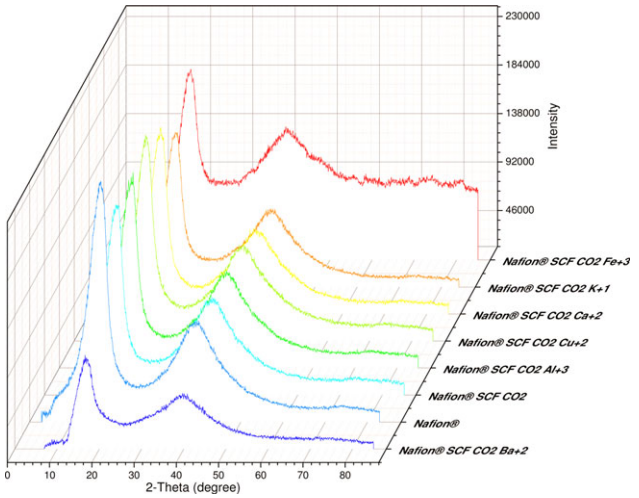

Figure 11. XRD patterns for Nafion® membranes processed with SCF CO_2 and exchanged with cation. [Color figure can be viewed in the online issue, which is available at wileyonlinelibrary.com.]

Nafion® processed with SCF CO_2 and then exchanged with calcium presented the largest value for the crystallinity of all the cations studied. These results agree with the DSC, TGA and SAXS results presented in the previous sections, where the reordering induced by the SCF CO_2 processing and the cation exchanged on the polymeric matrix changed the ionic cluster and matrix knee configuration (related to R_g). Table VIII summarizes the changes in crystallinity for all the Nafion® membranes studied.

Table VIII. Percent of Crystallinity of Nafion® Membranes

Membrane	Crystallinity (%)
Nafion®	26.9
Nafion® SCF CO_2	29.8
Nafion® SCF CO_2 Ba^{+2}	29.0
Nafion® SCF CO_2 Ca^{+2}	32.0
Nafion® SCF CO_2 Cu^{+2}	28.0
Nafion® SCF CO_2 Fe^{+3}	30.3
Nafion® SCF CO_2 Al^{+3}	25.1
Nafion® SCF CO_2 K^{+1}	23.6

Methanol Permeability

Methanol permeability for Nafion® membranes processed with SCF CO_2 and exchanged with cations are presented in Figure 13. The methanol permeability of Nafion® was reduced by 15% ± 2% compared with unprocessed Nafion® after processing with SCF CO_2. The permeability of small molecules through a membrane is defined as the product of a solubility coefficient and a diffusion coefficient. The limiting step of the diffusion process in a polymeric membrane is determined by the capacity of the compound to move through the free volume available in the system, which is related to morphology and crystallinity.[28] Nafion® processed with SCF CO_2 presents a reduction of the methanol permeability, one explanation for this is related to the results presented in the previous sections (e.g., TGA, DSC, SAXS), where the reordering induced by the SCF CO_2 processing on the polymeric matrix changed the morphology and crystallinity and produced a unique molecular configuration. This new molecular configuration inhibited the diffusion process reducing the methanol permeability.

The incorporation of cations significantly reduced the methanol permeability of the Nafion® membranes ever further. Nafion® SCF CO_2 with Cu^{+2} reduced by 32% ± 2% the methanol permeability with respect to unprocessed Nafion®. The incorporation of potassium reduced the permeability of methanol by 79% ± 2% and was the lowest methanol permeability for all the membranes studied.

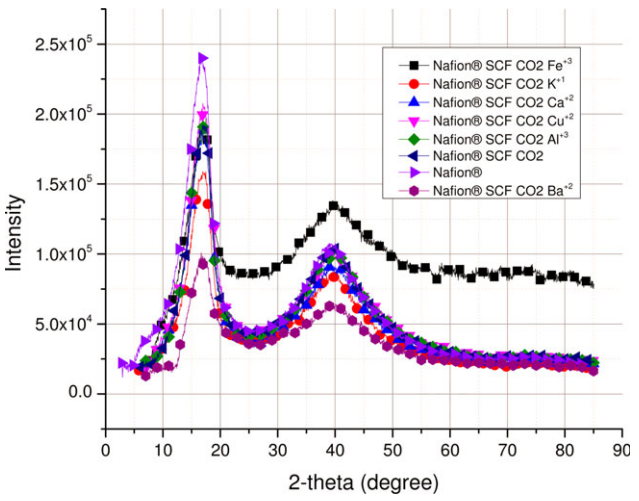

Figure 12. XRD patterns for Nafion® (—▶—) membranes processed with SCF CO_2 (—◀—) and exchanged with cation. (Frontal view): Fe^{+3} (—■—) K^{+1} (—●—), Ca^{+2} (—▲—), Cu^{+2} (—▼—), Al^{+3} (—◆—), Ba^{+2} (—●—). [Color figure can be viewed in the online issue, which is available at wileyonlinelibrary.com.]

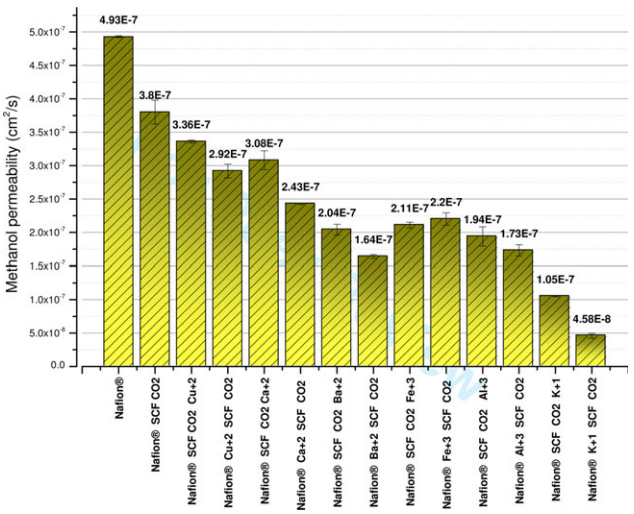

Figure 13. Comparison between methanol permeability for Nafion® processed with SCF CO_2 and then cation-exchanged. [Color figure can be viewed in the online issue, which is available at wileyonlinelibrary.com.]

Table IX. Methanol Permeability for Nafion® Membranes

Membrane	Methanol permeability $\times 10^7$ (cm^2 s^{-1})
Nafion®	4.93
Nafion® SCF CO_2	3.80
Nafion® SCF CO_2 Cu^{+2}	3.36
Nafion® SCF CO_2 Ca^{+2}	3.08
Nafion® SCF CO_2 Ba^{+2}	2.04
Nafion® SCF CO_2 Fe^{+3}	2.11
Nafion® SCF CO_2 Al^{+3}	1.94
Nafion® SCF CO_2 K^{+1}	1.05
Nafion® Cu^{+2} SCF CO_2	2.92
Nafion® Ca^{+2} SCF CO_2	2.43
Nafion® Ba^{+2} SCF CO_2	1.64
Nafion® Fe^{+3} SCF CO_2	2.20
Nafion® Al^{+3} SCF CO_2	1.73
Nafion® K^{+1} SCF CO_2	0.4

Table X. Proton Conductivity for Nafion® Membranes

Membrane	Proton conductivity; σ (s cm^{-1})
Nafion®	0.18 ± 0.006
Nafion® SCF CO_2	0.21 ± 0.009
Nafion® SCF CO_2 Cu^{+2}	0.017 ± 0.0007
Nafion® Cu^{+2} SCF CO_2	0.016 ± 0.0005
Nafion® SCF CO_2 Ca^{+2}	0.014 ± 0.002
Nafion® Ca^{+2} SCF CO_2	0.011 ± 0.001
Nafion® SCF CO_2 Ba^{+2}	0.010 ± 0.0002
Nafion® Ba^{+2} SCF CO_2	0.010 ± 0.001
Nafion® SCF CO_2 K^{+1}	0.016 ± 0.0004
Nafion® K^{+1} SCF CO_2	0.0068 ± 0.0001
Nafion® SCF CO_2 Al^{+3}	0.0038 ± 0.0002
Nafion® Al^{+3} SCF CO_2	0.0025 ± 0.0002
Nafion® SCF CO_2 Fe^{+3}	0.0061 ± 2.06E-05
Nafion® Fe^{+3} SCF CO_2	0.0481 ± 0.001

These results agree with the previously presented DSC, SAXS, and XRD results, where the variation of the methanol permeability for each cation is linked to the new sulfonic group conformation and the change in the crystallinity; each cation produced a unique morphology (related to its free volume) inhibiting the methanol permeability. Table IX presents the methanol permeability corresponding to each Nafion® membrane studied. Nafion® membranes exchanged first with cation and then processed with SCF CO_2 obtained the same tendency that Nafion® SCF CO_2 and then cation-exchanged but had a different methanol permeability value.

Proton Conductivity

Proton conductivity of Nafion® membranes processed with SCF CO_2 and cation exchanged are presented in Figure 14. The proton conductivity of Nafion® processed with SCF CO_2 compared with unprocessed Nafion® improved 14% ± 1%; after the processing with SCF CO_2. When the Nafion® membranes were exchanged with cations, the proton conductivity of these membranes was significantly reduced over one order of magnitude for all of them. Kim et al.[29] used molecular dynamics to study the transport mechanism of protons through the membrane. They proposed a transport of protons using hydrated sulfonic groups and suggested that the predominant mechanism consists in a series of Eigen–Zundel–Eigen or Zundel–Zundel transformations depending on: the sulfonic group, the water contained inside the membrane, and the polymeric structure.[29] The transport of certain compounds was also associated with their free volume available in the system.[28]

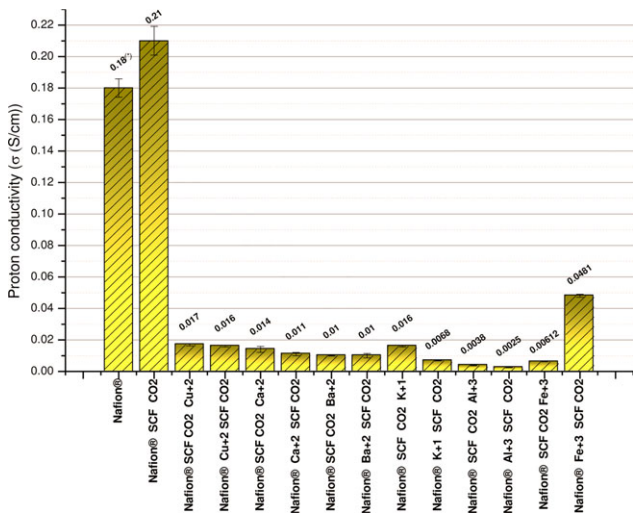

Figure 14. Comparison between proton conductivity for Nafion® processed with SCF CO_2 and then cation-exchanged and Nafion® cation-exchanged and then processed with SCF CO_2. [Color figure can be viewed in the online issue, which is available at wileyonlinelibrary.com.]

The processing with SCF CO_2 produced a reordering of the perfluorinated and perfluorovinylether chains in Nafion®. This is due to the affinity of perfluorinated and perfluorovinyl ether chains with CO_2, described by their polarizability per volume.[30] The cations interact with the ionic domains that inhibit the complex formation between the proton, water, and the sulfonic group described above. Also the transport was inhibited since each cation created new morphologies and changed the mobility of the proton through the membrane. These results are related to the changes induced by the SCF CO_2 and the cation on the molecular conformation of the polymeric chains in the membrane showed in the DSC, SAXS, and XRD experiments. Table X shows the results for all the membranes studied.

Figure 15 presents the normalized selectivities (proton conductivity/methanol permeability) for Nafion® membranes processed with SCF CO_2 and exchanged with cation (normalized with the selectivity of unprocessed Nafion®). SCF CO_2 processing alone presents the largest effect in selectivity. The incorporation of counter-ions significantly reduced the normalized selectivity of Nafion®, primarily due to the reduction in proton conductivity.

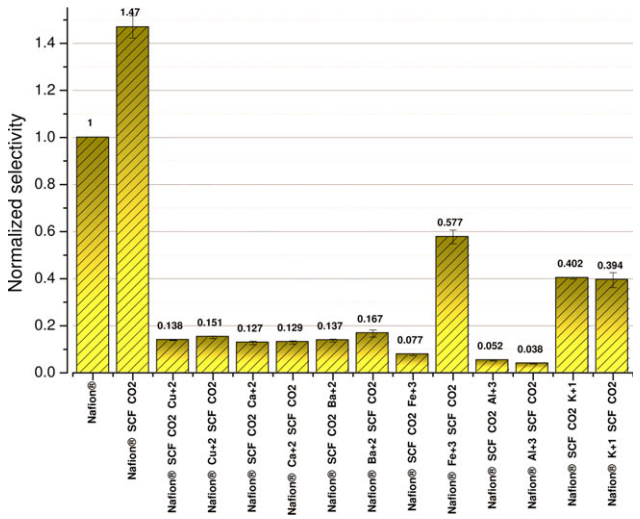

Figure 15. Normalized selectivities (proton conductivity/methanol permeability) for Nafion® membranes processed with SCF CO_2 and exchanged with cation. (Normalized with selectivity of Nafion® unprocessed). [Color figure can be viewed in the online issue, which is available at wileyonlinelibrary.com.]

CONCLUSION

Nafion® membranes were processed with SCF CO_2 and exchanged with different types of +1, +2, and +3 cations. The SCF processing with CO_2 promotes the transport of protons through the membrane and inhibits the methanol permeability. The molecular interaction between CO_2 and the fluorocarbon backbone makes a unique rearrangement in the polymer changing its water swelling, thermal degradation, crystallinity and morphology.

Nafion® processed with SCF CO_2 and cation exchanged inhibited both the transport of protons and methanol through the membrane. The incorporation of cations into Nafion® influences the ionic domains uniquely for each cation studied, but also influences the crystallinity, the morphology, and the water swelling, which are very important in the transport of protons through the membrane. Although the transport properties of both protons and methanol were reduced upon the incorporation of cations, suggesting some similarities in their transport mechanism, the magnitude of the changes were significantly different, suggesting that there are fundamental differences in their transport mechanism that can be further explored to create more selective membranes.

The best normalized selectivity (proton conductivity/methanol permeability, normalized with unprocessed Nafion®) was obtained using only SCF CO_2 (higher than unprocessed Nafion®). The use of cations significantly reduced the normalized selectivity of Nafion®, primarily due to the reduction in proton conductivity.

The processing order (SCF processing vs. cation substitution) shows that although the magnitude of the methanol permeability and proton conductivity are affected, the trends are primarily limited by the nature of the cation and not the order, suggesting that the physical changes induced by the supercritical fluid, although important; do not limit the chemical modifications.

ACKNOWLEDGMENTS

Financial support from the DOD through grants W911-NF-07-10244 and W911-NF-11-1-0486 is acknowledged. In addition the authors acknowledge the support of Prof. Danilo C. Pozzo, of the University of Washington, where the SAXS and XRD experiments were conducted (NanoTech User Facility of National Nanotechnology Infrastructure Network), Prof. Yossef A. Elabd of Drexel University, where the proton conductivity experiments were conducted and Prof. Carlos Rinaldi of the University of Puerto Rico at Mayagüez, where the DSC and FT-IR experiments were conducted. Finally, the authors acknowledge the help and support in the laboratory of: Sonia Avilés, Roberto Olayo, and Maritza Pérez.

REFERENCES

1. Elabd, Y. A.; Napadensky, E. *Polymer* **2004**, *45*, 3037.
2. Yang, B.; Manthiram, A. *J. Power Sources.* **2006**, *153*, 29.
3. Bai, Z.; Durstock, M. F.; Dang, T. D. *J. Membr. Sci.* **2006**, *281*, 508.
4. Yu Seung, K.; Michael, J. S.; William, L. H.; Judy, S. R.; James, E. M.; Bryan, S. P. *J. Electrochem. Soc.* **2004**, *151*, A2150.
5. Gebel, G.; Diat, O. *Fuel Cells.* **2005**, *5*, 261.
6. Neburchilov, V.; Martin, J.; Wang, H.; Zhang, J. *J. Power Sources* **2007**, *169*, 221.
7. Nagarale, R. K.; Shin, W.; Singh, P. K. *Polym. Chem.* **2010**, *1*, 388.
8. Jagur-Grodzinski, J. *Polym. Adv. Technol.* **2007**, *18*, 785.
9. Dardin, A.; De Simone, J. M.; Samulski, E.T. *J. Phys. Chem. B.* **1998**, *102*, 1775.
10. Akin, O.; Temelli, F. *J. Membr. Sci.* **2012**, *399*, 1.
11. Su, L.; Li, L.; Li, H.; Zhang, Y.; Yu, W.; Zhou, C. *J. Membr. Sci.* **2009**, *335*, 118.
12. Gribov, E. N.; Parkhomchuk, E. V.; Krivobokov, I. M.; Darr, J. A.; Okunev, A. G. *J. Membr. Sci.* **2007**, *297*, 1.
13. Pulido Ayazo, J. C.; Suleiman, D. *J. Appl. Polym. Sci.* **2012**, *124*, 145.
14. Sun, L.; Thrasher, J. S. *Polym. Degrad. Stab.* **2005**, *89*, 43.
15. Crank, J. In The Mathematics of Diffusion; Oxford University Press: Oxford, **1975**; Chapter 4, p 50.
16. Elabd, Y. A.; Napadensky, E.; Sloan, J. M.; Crawford, D. M.; Walker, C. W. *J. Membr. Sci.* **2003**, *217*, 227.
17. Grossi, N.; Espuche, E.; Escoubes, M. *Sep. Purif. Technol.* **2001**, *22*, 255.
18. Suleiman, D.; Napadensky, E.; Sloan, J. M.; Crawford, D. M. *Thermochim. Acta.* **2007**, *460*, 35.
19. Idupulapati, N.; Devanathan, R.; Dupuis, M. *J. Phys. Chem. A.* **2010**, *114*, 6904.
20. Heitner-Wirguin, C. *J. Membr. Sci.* **1996**, *120*, 1.
21. Grot, W. In Fluorinated Ionomers: PDL Fluorocarbon Series; William Andrew Publishing: Norwich, NY, **2008**; p 198.
22. Stefanithis, I. D.; Mauritz, K. A. *Macromolecules* **1990**, *23*, 2397.

23. Rosen, S. In Fundamental Principles of Polymeric Materials: SPE Monograph Series; Wiley Interscience Publication: New York, NY, **1993**; p 110.
24. Rubatat, L.; Rollet, A. L.; Gebel, G.; Diat, O. *Macromolecules* **2002**, *35*, 4050.
25. Narsimlu, N.; Siva Kumar, K.; Wu, C.-E.; Wu, C. G. *Mater. Lett.* **2003**, *57*, 2729.
26. Wei, Y.; Shen, L.; Wang, F.; Yang, W.-D.; Zhu, H.; Wang, Z.; Han, K. *Mater. Lett.* **2011**, *65*, 1684.
27. Li, L.; Su, L.; Zhang, Y. *Int. J. Hydrogen Energy* **2012**, *37*, 4439.
28. Budd, P. M.; McKeown, N. B.; Fritsch, D. *J. Mater. Chem.* **2005**, *15*, 1977.
29. Kim, E.; Weck, P. F.; Balakrishnan, N.; Bae, C. *J. Phys. Chem. B.* **2008**, *112*, 3283.
30. Johnston Keith, P.; Kim, S.; Combes, J. In Supercritical Fluid Science and Technology: ACS Symposium Series; American Chemical Society: Washington, DC, **1989**; Vol. 406, p 52.